Possible observation of multiple-particle tunneling in niobium tunnel junctions

C. L. Foden, N. Rando, A. van Dordrecht and A. Peacock
Astrophysics Division, Space Science Department of the European Space Agency, ESTEC, Noordwijk, The Netherlands

J. Lumley and C. Pereira
Oxford Instruments Scientific Research Division, Cambridge, England
(Received 8 April 1992; revised manuscript received 11 January 1993)

The I-V characteristics of strongly coupled symmetric niobium-based superconducting tunnel junctions are found to display steplike structures at voltages less than the gap voltage $2\Delta/e$. A thorough investigation into the influences of magnetic-field and temperature variations on the structures has been performed. In addition, measurements have been made that allow the homogeneity of the junction barrier to be determined. The experimental results indicate that the structures arise due to either self-coupling, multiple Andreev-reflection processes or multiple-particle tunneling. The data have been analyzed in terms of each of these theories. The results of this analysis appear to indicate that multiple-particle tunneling is the mechanism most likely to be responsible for the subgap structures. If this is the case, this would indicate that three-particle tunneling has been observed in niobium-based junctions. Specific features in the structures are also observed; the current steps do not appear at exactly the voltages expected, and some steps are sharper than others. A modified version of the theory describing multiple-particle tunneling is also presented. It is found that this model is in good agreement with the experimental data. In addition, it is able to describe all features of the structures and indicates the presence of two different, resolved gaps in the superconducting region next to the junction barrier.

I. INTRODUCTION

Recent investigations into the properties of strongly coupled (thin oxide barrier), superconducting tunnel junctions (STJ's) have revealed subgap structures in the current-voltage (I-V) characteristics. These structures are found to occur at one half and one third of the measured gap voltage $2\Delta/e$.

Subgap structures in the I-V characteristic (i.e., currents in excess of the thermal current) may occur for a variety of reasons.[1–5] However, the voltage location of the structures indicates that one of several well-known mechanisms is responsible: multiple-particle tunneling,[2] multiple Andreev-reflection processes,[5,6] or self-coupling.[3]

Multiple-particle tunneling (MPT) corresponds to the simultaneous tunneling of two or more (n) electrons.[7–9] In any such process, two quasiparticles are generated, and n quasiparticles are transferred across the barrier. Multiple Andreev reflection (MAR) is a process by which particles can tunnel across the barrier at energies lower than the gap.[4] This occurs via a reflection mechanism occurring under the influence of a discontinuity in the pairing potential. Self-coupling (SC)[7,8,10,11] is an effect produced by the ac Josephson current: the photons emitted at the Josephson frequency may either assist tunneling directly, or may break Cooper pairs. The major features of the subgap structures resulting from these effects is well documented elsewhere,[5,8,12] so only a summary is included in this paper.

Subgap excess currents have been reported previously,[8–10,13–15] yet it is still unclear as to which effect is the one most likely to be causing them. Both MPT and SC effects produce subgap structures at voltages corresponding to $2\Delta/n$ (n integer). However, the form of the structures can be different in these two cases, so it could be possible to distinguish between MPT and SC: for strongly coupled junctions, MPT theory predicts steplike structures, whereas SC theory predicts resonancelike peaks.[12] An additional variation occurs in the magnitude of the structures: MPT theory predicts a far more rapid decrease in magnitude with increasing n than does SC theory, resulting in a larger number of structures being observable if SC is the effect responsible.[12]

MAR, for ultrathin barriers, predicts structures with onset voltages which are not exactly equal to $2\Delta/n$, but which are shifted.[5] The magnitude of the peaks in this case does not fall off as rapidly as for MPT, but falls more rapidly than in the SC case.

In this paper, the experimental and theoretical results from several different devices are presented. The main conclusion is that the subgap structure seen is most probably due to MPT, in which case three-particle tunneling has been observed in niobium-based STJ's, although it is not possible to refute the other two mechanisms entirely. In addition, proposals are made for future experiments which could contribute further to the understanding of the results presented in this paper.

II. EXPERIMENTAL DETAILS

Since it is the properties of the subgap current which are of interest, devices were fabricated with highly transmissive, yet leak-free, barriers, such that any subgap structures would be observable. Many devices consis-

tently display, to some degree (depending upon the transmissivity of the barrier) the characteristics reported here, but the results from three only are presented; two (B and C) to demonstrate reproducibility on a chip, and one (A) to demonstrate reproducibility between chips.

The geometry of the junctions under investigation is described in detail elsewhere.[16] In summary, eight devices are fabricated on each chip from a single trilayer of Nb/Al/AlOx/Nb: the lower layer is epitaxial niobium capped with a thin layer (50 Å) of partially oxidized aluminium which forms the potential barrier. The upper layer is polycrystalline niobium. Details of fabrication and processing may also be found elsewhere.[16] The devices all have an upper layer and barrier area of 144 μm^2, and a lower layer of area 400 μm^2. A summary of the additional relevant properties of the three devices investigated is given in Table I.

I-V curve data were taken as functions of both temperature and magnetic field. In addition to *I-V* characterization, the capacitance of the devices was determined, giving the barrier thickness via $C = \epsilon_0 \epsilon_r A/d$. A detailed description of the experimental configuration can also be found in Ref. 16.[17]

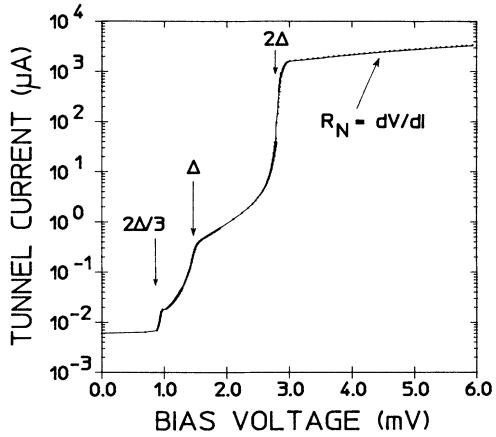

FIG. 1. The complete *I-V* characteristic for one of the devices (A), taken at 1.23 K. The other two devices have similar characteristics. Note the switching of the current back to the Josephson current below the lowest data point (at 0.7 meV). This feature arises as the system is current driven, and, for accurate step amplitude measurement, must occur away from the step region, as shown in the figure.

III. RESULTS

A. *I-V* characteristics

The complete *I-V* characteristic for one device (A) is shown in Fig. 1. The structures seen at Δ and $2\Delta/3$ are clearly visible for all three devices. A series of high-resolution fits to the data around the $2\Delta/3$, Δ and 2Δ regions are shown in Figs. 2(a)–2(c), respectively. The differentials of the data are also shown, and may be used to derive both the current steps $\delta I_{2\Delta/n}$ and the gaps $2\Delta_{2\Delta/n}$ corresponding to each step. The effects on the Δ and $2\Delta/3$ points of increasing the temperature and magnetic field are shown in Figs. 3 and 4, respectively, for device B.

The peaks become slightly smeared as the temperature is increased, but do not appear to be strongly influenced by the magnetic field. Reproducibility of the structures is good in that they are always present, regardless of the magnetic field strength, as long as the thermal current is not too large. There can however be variations in the step amplitude (5% for the Δ point, 30% for the $2\Delta/3$ point), during repetitions of the experiment, with or without a change in the magnetic field. This variation seems to be somewhat related to the magnitude of the DC Josephson current which becomes more difficult to stabilize and to suppress completely when the thermal current is low. Since the system is current driven, it is important to note that regions of negative differential resistance would be seen only via the hysteretic behavior of the current around that region. The absence of any such behavior, particularly when the Josephson current amplitude is less than that of the current step, indicates that the structures are steplike rather than cusplike or resonancelike. The amplitudes of the current steps, $\delta I_{2\Delta/n}$, are summarized in Table II, along with their corresponding half-gaps $\Delta_{2\Delta/n}$, obtained from the maxima of the differentials. As can be seen from Table II, for each device, the values for the gap 2Δ, inferred from the voltages at which the three steps occur, are not equal. Rather, there appear to be two different values of gap for each device. This is an important feature which will be discussed later. In addition, there appears to be a somewhat random variation in the step width.

There are additional features also visible in some of the *I-V* curves, namely, steps of much smaller amplitude, visible as "shoulders" to the main steps. These features are easily suppressed by varying the magnetic field, and so are probably not related to the main steps, but rather are due to resonances within the device itself.

B. Capacitance measurements

The capacitance of the devices was determined from the hysteresis of the *I-V* curve, on the basis of the re-

TABLE I. The principal characteristics of the devices. $t_{t/b}$ = thickness of top and/or bottom layer, $V_m = I_c^{exp} R(2\text{ mV})$, quality parameter obtained at 4.27 K, R_N = normal resistance of junction, R_D = dynamic resistance (at 0.5 mV), and $2\Delta/e$ = gap voltage. N.B. values were obtained at 1.23 K unless otherwise specified.

Device	t_t (Å)	t_b (Å)	V_m (mV)	R_N (Ω)	R_D (kΩ)	$2\Delta/e$(mV)
A	850	500	96	1.7	≥ 200	2.94
B	850	250	81	2.2	200	2.92
C	850	250	68	2.3	≥ 100	2.94

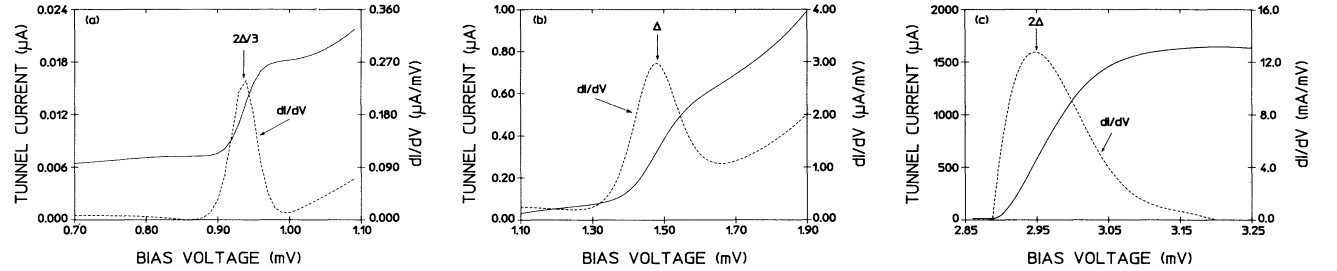

FIG. 2. The best fit spline function to the I-V data shown in Fig. 1 around (a) the $2\Delta/3$ region, (b) the Δ region, and (c) the 2Δ region, along with the differentials dI/dV.

sistively shunted model.[16,18,19] Since $C = \epsilon_0\epsilon_r A/d$, the barrier thickness could be evaluated. The measurements were taken with the device both positively and negatively biased, giving two values of barrier thickness d_+ and d_-. The average of these two results, d, is quoted in Table II. The measurements indicate, for all three devices, a barrier thickness of less than 10 Å. It should be noted that although the values obtained are of the right order of magnitude, based on the aluminium oxidation time, the accuracy of this measurement is not expected to be extremely high. The model used tends to underestimate barrier thicknesses,[20] since the capacitance tends to be overestimated. It is therefore anticipated that d could actually be double the values quoted, and thus the tabulated values should be regarded as a lower bound on the thickness of the insulating region. The value taken for ϵ_r is taken to be equal to 10.5, see Ref. 16.

Evaluation of the errors in the values of $\delta I_{2\Delta/n}$ is difficult: there are clearly a range of values obtained experimentally, and determination of a particular value from the differential leads to further errors. The principal uncertainties in δI were found to be related to both the experimental current fluctuations over a small change in bias voltage, and to the estimation of the current step via the differential. The errors in Δ are primarily related to systematic uncertainties associated with the bias voltage and the Josephson current. The errors quoted are probably overestimates.

Since the barriers are rather thin, it was considered important to make additional measurements to examine the overall barrier uniformity and quality.

C. Josephson critical current

Measurement of the critical Josephson current as a function of magnetic field provides a measure of barrier uniformity. Figure 5 shows the results for one device (A). The data in this case could be fitted reasonably well assuming a uniform tunneling current distribution and a geometrically square tunneling region, with negligible edge effects (leaks). Other, more complex, models could not provide any improvement in the fit. As might be expected in such junctions, the current does not actually go to zero. This feature is obscured in Fig. 5 due to the scale and to the presence of the line showing the theoretical fit. It is of interest to note that similar models of previous junctions required the incorporation of edge effects, or leaks, via the assumption of a very non-uniform current distribution across the film.[16] The earlier junctions, however, were fabricated with a different mask, and were far less well defined geometrically than the present junctions. It is therefore difficult to discuss whether edge effects were in fact present in the earlier junctions, or whether the junction shape itself was the major influence on the Josephson current behavior.

D. Thermal current

The variation of the thermal current with temperature provides a measure of the leakage current (due to barrier pinholes) in a device. The inset of Fig. 5 shows the thermal current at 0.5 mV for device A. The variation in the current follows the predicted BCS variation corresponding to a half-gap of $1.42 \pm .02$ mV, in reasonable agreement with the previously obtained values of Δ (see Table II). The leakage current is extremely small, of order $1nA$ at 1.23 K, indicating a very high quality barrier.

IV. THEORY

The expression for the amplitude of the current density step of the nth peak, according to MPT theory is[8,12]

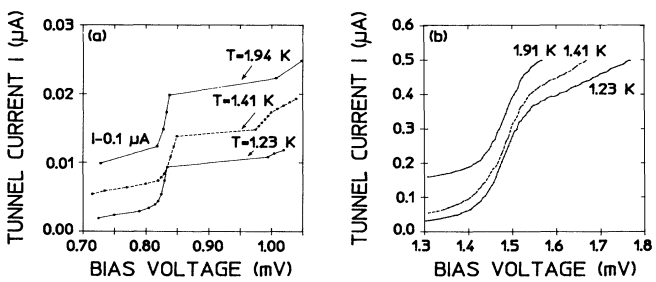

FIG. 3. The I-V characteristics of device B around (a) the $2\Delta/3$ region and (b) the Δ region for various device operating temperatures. The magnetic field was held constant at around 630 Gauss.

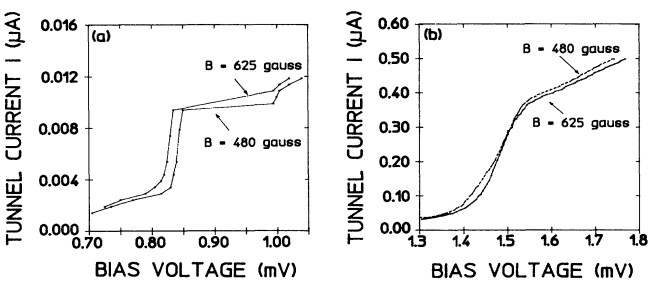

FIG. 4. The I-V characteristics of device B around (a) the $2\Delta/3$ region and (b) the Δ region for two different magnetic fields. All measurements were taken at a temperature of 1.23 K.

TABLE II. The parameters derived from the I-V data.

Device	$\delta I_{2\Delta}$ (μA)	$\frac{\Delta_{2\Delta}}{e}$ (mV)	δI_{Δ} (μA)	$\frac{\Delta_{\Delta}}{e}$ (mV)	$\delta I_{2\Delta/3}$ (nA)	$\frac{\Delta_{2\Delta/3}}{e}$ (mV)	d (Å)
A	1560±50	1.47±0.05	0.59±0.02	1.48±0.01	11.0±0.3	1.40±0.01	5
B	1180±50	1.46±0.05	0.36±0.02	1.49±0.01	6.7±0.3	1.26±0.01	5
C	1070±50	1.47±0.05	0.33±0.02	1.48±0.01	2.6±0.3	1.23±0.01	6

$$\delta J_n(2\Delta/n) = \frac{e\Delta}{4\pi\hbar d^2}\tanh\left(\frac{\beta\Delta}{2}\right)\left(\frac{e^{-s}}{16}\right)^n\left(s+\frac{1}{n}\right) \times\left[\left(\frac{2}{n!}\right)\left(\frac{n}{2}\right)^n\right]^2; \quad (1)$$

here $s = 2kd$, $k = \sqrt{2m_eV_b}/\hbar$ in Å^{-1}, d =barrier thickness, V_b =barrier height, m_e =free electron mass and $\beta = 1/(k_BT)$.

The amplitude of the structures is therefore proportional to $|T|^{2n}$ for MPT, where T is the tunneling matrix element. For SC however, the amplitude is thought to be proportional to $|T|^2$, resulting in a far less rapid variation in the size of the current peaks. For MAR, the peak size for the single-particle current peak is also proportional to $|T|^2$, with both the two- and three-particle peaks proportional to $|T|^4$. Using Eq. (1), and assuming a perfectly uniform barrier, expressions for the amplitudes of the various current peaks may be obtained. Subsequent comparison with the experimentally determined amplitudes indicates that current steps measured at submultiples of the gap are in excess of those which would be expected in accordance with the current step at the gap (see Table II and Ref. 12). For this reason, the normal procedure is to assume the barrier is divided into thin (d_2) and thicker (d_1) regions, both regions transmitting the single-particle current, but only the thinner regions, due to their higher transmissivity, carrying the multiple-particle currents.[2,12] Thus the actual current step amplitudes will be given by equations of the form

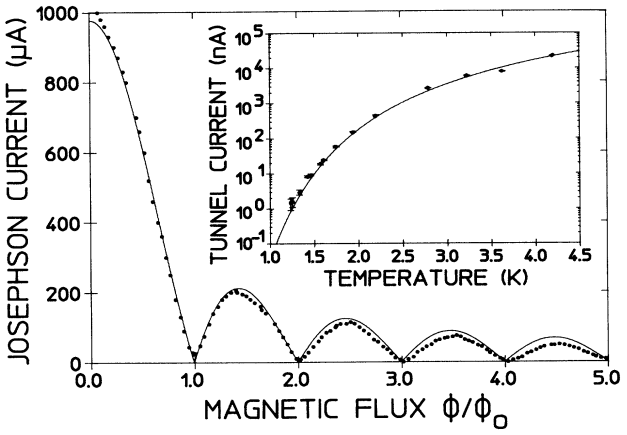

FIG. 5. The variation of the maximum Josephson current as a function of magnetic flux for device A at 4.2 K. The data points are reasonably well described by the theoretical uniform barrier model (solid line). The inset shows the variation of the thermal current as a function of temperature at 0.5 mV for the same device. The solid line is the thermal current, based on the BCS theory.

$$\delta I_1 = \frac{e\Delta}{4\pi\hbar}\left\{\frac{A_1}{d_1^2}\left(\frac{e^{-s_1}}{16}\right)(s_1+1)+\frac{A_2}{d_2^2}\left(\frac{e^{-s_2}}{16}\right)(s_2+1)\right\} \quad (2)$$

and

$$\delta I_{n\geq 2} = \frac{e\Delta}{4\pi\hbar}\frac{A_2}{d_2^2}\left(\frac{e^{-s_2}}{16}\right)^n\left(s_2+\frac{1}{n}\right)\left[\left(\frac{2}{n!}\right)\left(\frac{n}{2}\right)^n\right]^2. \quad (3)$$

Since $\tanh(\beta\Delta/2) \approx 1$, it is omitted. A_1 is the area of the thicker region, and A_2 that of the thinner. It will be seen later that this simple model must be modified in order to describe additional features of the I-V data.

Subsequent calculations using Eqs. (2) and (3) and the experimental values for the amplitude ratios of the different current steps give theoretical values both for s_2 and s_1, from which the thickness of the thicker region at least may be inferred. The thickness of the thinner region is left unspecified: the potential barrier provided by a very thin region is expected to be lower than that for the thicker regions, but its exact height is unknown.

The barrier wave-vectors k are chosen to correspond to a barrier height of around 1 eV (for the thicker region), which is considered to be a reasonable value for aluminium oxide, previously estimated values range from 0.32 to 1.9 eV (see Ref. 16 and references therein). However, since the barrier is so thin, it may well be that a lower value of k would be more suitable. (Lower values of k correspond to thicker barriers, since $2kd$ is constant.) Even so, the values of d_1^{th} are very close to or within a factor 2 of those derived from the capacitance measurements. (See Table III.)

Using a range of values for the barrier height for the thin region (corresponding to $0.1 \leq k \leq 0.6$), an estimate of the area of the thinner region can be made. This area is found to be always less than 0.1% of the total barrier area. Since the barrier consists virtually entirely of thicker regions, it is the value of d_1 which must be compared with the experimentally obtained value for the barrier thickness.

The above model neglects contributions to the two- and three-particle currents from the thick regions. However, using the values of s_1 obtained, it may be seen that this assumption is not valid for the two-particle current; for all three junctions the contributions from both regions to the current step at Δ must be included. The model must therefore be extended to allow for, at least, two-particle tunneling through the thicker regions.

There are two further important features of the I-V curves which are also not described by the above model, but must be included. The first is that the single-particle current peak occurs at a voltage corresponding to a half-

TABLE III. The theoretical values of barrier thickness and s_2 obtained using the simple model described by Eqs. (2) and (3).

Device	k (Å^{-1})	d_1^{th} (Å)	s_2^{th} (Å)
A	0.5	7.8	1.4
B	0.5	8.0	1.4
C	0.5	8.2	2.2
A	0.6	6.8	1.4
B	0.6	7.0	1.4
C	0.6	7.1	2.2

gap of, say, Δ_1, whereas that of the triple-particle peak occurs at a voltage corresponding to Δ_2, where $\Delta_2 < \Delta_1$. The second feature is that the one- and three-particle current peaks are fairly sharp compared with that at the two-particle point. It may therefore be inferred that there are two values of Δ, one corresponding to the thinner barrier regions Δ_2, and one to the thicker Δ_1. The sharpness of the peak then indicates whether the tunneling is occurring at one particular value of the gap, or over a range. Thus it would appear that the three-particle current is mainly due to transmission through the thin parts of the barrier, the single particle occurring mainly through the thicker parts, and the double particle over a range. This means that the devices are able to resolve the two different gaps via the mechanism involved in producing the subgap structures.

The proposals outlined above may be incorporated into Eq. (1), such that a general expression for the amplitude of the nth step is as follows:

$$\delta I_n = \frac{e}{4\pi\hbar}\left\{\mathcal{X}_1\left(\frac{e^{-s_1}}{16}\right)^n\left(s_1+\frac{1}{n}\right) + \mathcal{X}_2\left(\frac{e^{-s_2}}{16}\right)^n\left(s_2+\frac{1}{n}\right)\right\} \times\left[\left(\frac{2}{n!}\right)\left(\frac{n}{2}\right)^n\right]^2 \quad (4)$$

where

$$\mathcal{X}_i = \frac{A_i\Delta_i}{d_i^2}$$

with $i = 1, 2$ and $\Delta_{1,2}$ obtained from the data.

The set of simultaneous equations for the three current steps may be solved for a suitable range of barrier wave-vector values for the thicker region. The solutions give the corresponding ranges for s_2, d_1 and the percentages of each of the one-, two-, and three-particle currents transmitted by each of the thin and thick regions. The results are summarized in Table IV.

The values of d_2 are again left unspecified since the barrier height corresponding to a very thin region is unknown. The solutions indicate, as anticipated, that the three-particle current is transmitted by the thinner region of the barrier, whereas the one- and two-particle currents are transmitted by both regions. This feature enables the two gaps Δ_1 and Δ_2 to be resolved.[21] The corresponding thinner regions are thought to have areas of less than 10^{-3}% of the total for devices A and B, and less than 10^{-2}% for device C. The three values of d_1 obtained are in good agreement with those obtained experimentally. The values of s_1 and s_2 obtained also imply that the current steps at $2\Delta/n$ with $n \geq 4$ would be of too small an amplitude to be detected above the thermal current. However, it is also important to note that, because of the switching of the quasiparticle current at around $1n$A due to incomplete suppression of the Josephson current (see Fig. 1), observation of any further steps would be extremely difficult.

In support of one of the hypotheses on which this model is based, it is worth noting that, according to the McMillan theory,[22] the gap induced in the aluminium density of states by the proximity of the superconducting niobium is given by

$$\Delta E = \Delta_{Al} + \frac{\hbar v_F}{4}\left(\frac{\sigma}{B}\right)\frac{1}{\lambda_{Al}}. \quad (5)$$

Δ_{Al} is the half-gap in aluminium, λ_{Al} is the thickness of the aluminium, and v_F is the Fermi velocity in aluminium. σ/B is a constant for the device, dependent upon quasiparticle transmission across the Nb-Al interface. The total thickness of aluminium deposited is known to be 50±10 Å, therefore using the two values of Δ obtained experimentally for each device, values for the thinner barrier regions may be evaluated, and thus via s_2, estimates for the values of k for the thinner regions may be made. Within the errors quoted earlier, d_2 is thought to be around 2 Å for devices A and B, and around 3 Å for device C corresponding, as stated earlier, to reduced values of k in the thinner regions. However, these results should be treated with caution, and will be discussed further in the next section.

V. DISCUSSION AND CONCLUSIONS

According to the results of the theoretical analysis, the thicker regions of the barrier are rather thin, and the thinner regions would appear to be extremely thin. However, it is anticipated that, with very thin oxide barriers, it is no longer possible to discuss actual thicknesses,[5] but rather effective thicknesses. Assuming the thinner regions to be homogenously distributed across the barrier, then since the areas of the thinner regions are so small, the areal density of the thinner regions is extremely low, at most one part in 10^4 is affected, however, this will still introduce further stresses and strains into the system as a whole. It is clear that the physical structure of the

TABLE IV. Theoretical values for d_1, s_2 and the percentages of each of the n-particle currents transmitted by the thicker region of the barrier, $I_{2\Delta/n}(d_1)$, obtained from the solution of Eq. (4), with the barrier wave vector k set at 0.5 Å^{-1}.

Device	$I_{2\Delta}(d_1)$	$I_{\Delta}(d_1)$	$I_{2\Delta/3}(d_1)$	d_1^{th} Å	s_2
A	97%	6%	$< 10^{-2}$%	7.8	1.3
B	98%	6%	$< 10^{-2}$%	8.0	1.3
C	95%	5%	$< 10^{-2}$%	8.1	2.2

whole insulating region will be quite different to that of the bulk insulator: neighboring atoms may have a greater separation than normal, resulting in weaker bonding due to the reduction in wave function overlap, particularly in the neighborhood of the thinner areas. In addition, the properties of such a structure would be quite different from those of the bulk: it would appear more realistic to discuss the effective thickness of the barrier; that is the one the barrier appears to have, according to its electrical properties, which is not neccessarily simply related to its "actual" thickness. The thicknesses obtained experimentally and theoretically should therefore be interpreted in this way. It may perhaps even be desirable to omit discussion of the thickness of the thinner region entirely, using only s_2,[12] which is perhaps a more physically meaningful parameter. It is difficult to discuss what kind of potential barrier the insulating region will provide, however, the fact that the theoretical model can describe the experimental data quite adequately, indicates that it is at least possible to describe the layer as a barrier with an effective thickness. It is of interest to note that there is a slight discrepancy between the MPT results contained here, and standard tunneling theory results for the resistance of the barrier. However, the strong (exponential) dependence of the resistance on both the barrier height and wave vector means that small errors obtained in either of these values can result in much larger errors in the values of the resistance. The presence of the inconsistency does, however, imply that the simple rectangular barrier models used in both the tunneling theory and MPT require modification in order to improve the agreement with the data.

Since the barriers are thin, it would seem possible that pinholes could exist in the devices. However, the thermal current variation with temperature down to 1.23 K, and the critical current variation with magnetic field imply only a very low level of leakage. The theoretical results indicate that the thinner regions have an area of, at most, 0.01% of the total barrier area and in fact contribute less than 5% to the single-particle current. So, it may be concluded that even though they are thin, the barriers are still of very high quality.

The three different devices tested were all fabricated to the same specifications with regard to the barrier. Two devices are from the same chip (B and C), and the other (A) is from a separate chip. The extremely good reproducibility of the step structure from device to device, both in amplitude and form, is also a good indication of the nature of the cause of the structures. If they were due to SC via pinholes and shorts in the system, good reproducibility would not be expected. In conjunction with the information obtained theoretically, it may be concluded that the devices are virtually leak free.

The lack of dependence on magnetic field of the step amplitudes and positions eliminates the possibility that they are due to any resonances within the system,[22] and the lack of any temperature dependence indicates that they are in no way due to some form of thermally assisted process.

The steplike shape and the rapid decrease in amplitude of the subgap structures, coupled with the information contained in the above discussion indicate that SC is an unlikely cause. The success of the theoretical model in describing the I-V data, in terms of a barrier with two regions of different effective thicknesses, and the good agreement between the theoretically and experimentally obtained values of these thicknesses, indicate that MPT is a possible candidate. More evidence which would appear to discount the SC in favor of the MPT or MAR explanations is that a step at Δ, identical in form to those reported here, is often seen in less strongly coupled devices, as shown in Fig. 6. In such devices there is absolutely negligible leakage current, the Josephson current is easily suppressed and the thermal current is well behaved, generally indicating a virtually imperfection-free device. Such devices do not display the step at $2\Delta/3$, but the magnitudes of the $2\Delta/2$ step in these cases indicate that indeed the three-particle step, if it were due to MPT or MAR, should not be visible.

Quantitative analysis in terms of the MAR theory as it stands is difficult. Qualitatively, it provides another explanation for all the features of the observed sub-gap structures. In particular, this theory is able to account for the fact that the three voltages at which steps are found in the data do not correspond exactly to $2\Delta/n$, but are offset, which as outlined in the Introduction, is a feature of this theory. However, quantitatively, MAR gives the offset of the peak voltage from $2\Delta/3$ to be positive. In the data presented here, the offset is negative, that is the peaks occur at voltages lower than expected from the value of Δ. An obvious point in favor of this theory as an explanation is that it obviates the need for regions of reduced barrier thickness (in the theory of MAR, both the $n = 2$ and $n = 3$ peaks are proportional to $|T|^4$), and therefore appears to give more physically acceptable results.

MPT theory, with the incorporation of two different

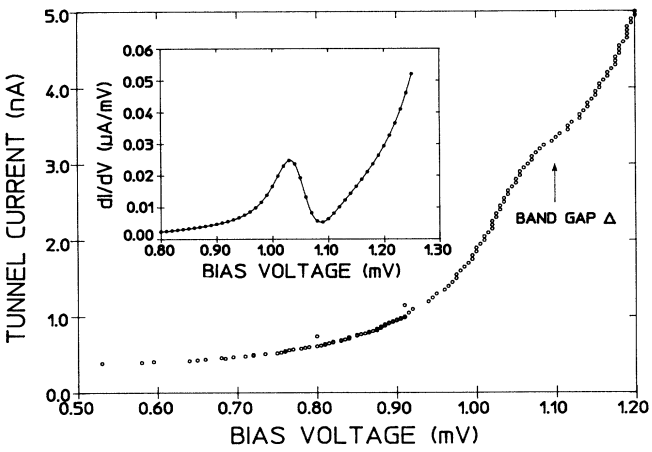

FIG. 6. The I-V characteristic around the Δ region for a device with a higher normal resistance (57 Ω). The half-gap voltage for this device is low (1.05 mV), since it has a greater thickness of aluminium (130 Å). The differential, shown in the inset, clearly indicates the step at Δ. The step at $2\Delta/3$ would be too small to be detected.

band gaps and the notion of two "effective" barrier thicknesses can describe the data extremely well. The presence of two regions of different thickness present in the barrier is supported by the measurements of the Josephson current as a function of magnetic flux. Additionally, such barriers are known to have a rough, pitted surface. MAR theory, with no modifications, is able to provide a qualitative explanation for all features of the data, quantitatively it may not. It appears therefore, of the three candidate effects, MPT is the one most likely to be causing the subgap structures. However, since the type of experiments performed measure macroscopic quantities which are determined by the underlying quantum nature of the system, it would appear impossible, without further experimentation, to determine the true nature of the origin of the effects seen.

In summary, if the subgap structures observed arise due to MPT, then an observation of three-particle tunneling has been made in niobium-based superconductors. Correspondingly in this case, the two regions of the barrier, thick and thin, have different but resolved (by the tunneling mechanism), values of gap.

However, it should be noted that it is also not possible to eliminate the SC explanation entirely. In both devices, the Josephson current is very large, and quite difficult to suppress totally, indicating that there may well be an extremely small amount of leakage within the system, and in fact the presence of shorts may well favor the SC mode.[12]

Future theoretical work will include development of the MAR theory in order to attempt to describe the features of the data described here in terms of Andreev scattering. Future experimental work will investigate the subgap structure of asymmetric devices, that is junctions fabricated from two different superconductors: A and B. The $n = 2$ structures in this case appear at Δ_A and Δ_B. For the case of $\Delta_A \leq \Delta_B$, the peak at Δ_B will dominate for MPT, and that at Δ_A if SC is the responsible effect. It is of interest to note that in the junctions discussed in this paper, Δ_A, say, has two components: Δ_1 ($\approx \Delta_B$), and Δ_2. The small difference between Δ_1 and Δ_2 would presumably not give rise to two separate peaks, but a smeared single one, increasing in amplitude with voltage, precisely as was seen at the two-particle point. (It should be noted at this point that no peak at the gap difference is seen in our data, this is due to the fact that the system is current driven, and so insensitive to features at such low voltages.) It is also hoped that, in the future, measurements of barrier thickness via Fiske step measurements can be made, since this method is far more accurate than the technique used here. In addition, it would be of interest to repeat the experiments of Giaver and Zeller,[10] in which the dependence of the peak height on the barrier transmission coefficent was tested, for reasons outlined earlier. Such experiments should reveal the true nature of the origin of the subgap structure.

[1] M.D. Fiske, Rev. Mod. Phys. **36**, 221 (1964).

[2] J.R. Schrieffer and J.W. Wilkins, Phys. Rev. Lett. **10**, 17 (1963).

[3] N.R. Werthamer, Phys. Rev. **147**, 255 (1966).

[4] T.M. Klapwijk, G.E. Blonder, and M. Tinkham, Physica **109 and 110B**, 1657 (1982).

[5] Gerald B. Arnold, J. Low Temp. Phys. **68**, 1 (1987).

[6] A.F. Andreev, Zh. Eksp. Teor. Fiz. **46**, 1823 (1964) [Sov. Phys. JETP **19**, 1228 (1964)].

[7] J.W. Wilkins, *Tunnelling Phenomena in Solids* (Plenum, New York, 1969).

[8] L.E. Hasselberg, M.T. Levinson, and M.R. Samuelson, Phys. Rev. B **9**, 3757 (1974).

[9] C.J. Adkins, Philos. Mag. **8**, 1051 (1963).

[10] I. Giaver and H.R. Zeller, Phys. Rev. B **1**, 4278 (1970).

[11] S. Strassler and H.R. Zeller, Phys. Rev. B **3**, 226 (1971).

[12] P. Mukhopadhyay, J. Phys. F **9**, 903 (1979).

[13] B.N. Taylor and E. Burstein, Phys. Rev. Lett. **10**, 14 (1963).

[14] R. Monaco, R. Cristiano, L. Frunzio, and C. Nappi, J. Appl. Phys. **4**, 1888 (1992).

[15] E.C.G. Kirk, M.G. Blamire, R.E. Somekh, J.E. Evetts, D. van Vechten, and M.N. Lovellette, IEEE Trans. Mag. **27**, 3137 (1991).

[16] N. Rando, A. Peacock, A. van Dordrecht, C.L. Foden, R. Engelhardt, B.G. Taylor, J. Lumley, and C. Pereira, Nucl. Instrum. Methods **A313**, 173 (1992).

[17] Two recent improvements are, however, worthy of mention: the first is that the magnetic field is now produced by a small internal superconducting magnet providing a well defined and oriented field, and a higher maximum field of 0.2T. Second, the *I-V* data is now acquired with a very low noise and low frequency unit, based on a 16 bit ADC-DAC scheme, still utilizing the electronically compensated two wire technique, but now allowing high-resolution measurements in the mA to pA range to be performed.

[18] A. Barone and G. Paterno, *Physics and Applications of the Josephson Effect* (Wiley, New York, 1982).

[19] D.E. McCumber, J. Appl. Phys. **39**, 2503 (1968).

[20] A.W. Kleinsasser and R.A. Buhrman, Appl. Phys. Lett. **37**, 841 (1980).

[21] Note that, in general, the barrier thickness and/or aluminium thickness are such that the variation in the two values of Δ is negligible.

[22] W.L. McMillan, Phys. Rev. **175**, 537 (1968).